2026 IEEE/SICE International Symposium on System Integration (SII)
January 11-14, 2026. Cancún, México

Human-in-the-Loop Control of a Soft Pneumatic Exosuit for Step Width Guidance via Hip Abduction/Adduction

Jinnosuke Kamimura[1,†], Tetsuro Miyazaki[1,†] and Kenji Kawashima[1]

Abstract— **The constraints of cable-driven actuation have largely limited mediolateral (ML) assistance from soft exosuits to hip abduction. To address this limitation, we developed a soft pneumatic exosuit actuated by pneumatic artificial muscles (PAMs) capable of providing bidirectional assistance to both hip abduction and adduction to guide the wearer's step width. Given the challenges in accurately modeling PAM-driven systems, we propose a Human-in-the-Loop (HIL) approach that treats the human-exosuit system as a black box and uses Bayesian optimization to tune control parameters. In walking experiments with two healthy participants, the proposed HIL framework successfully identified participant-specific PI gains during the parameter tuning session. In the subsequent validation, the controller based on the optimized gains reduced the mean step-width RMSE by** 43.4 % **for Participant 1 and** 26.8 % **for Participant 2 compared with the condition without assistance. The optimized gains also provided an additional improvement of** 3.76 % **for Participant 1 and** 1.07 % **for Participant 2 relative to the controller with initial gains. These results indicate that the proposed approach offers a practical method for personalizing assistance in soft pneumatic exosuits and contributes to the development of devices that enhance ML balance.**

I. INTRODUCTION

A. Background

Research on wearable robots for walking assistance has been actively conducted [1]; however, most existing studies have focused on assistance in the anteroposterior (AP) direction. In contrast, maintaining stability during walking also requires control of balance in the mediolateral (ML) direction [2]. Older adults and patients with neurological disorders often exhibit diminished ML balance control, increasing the risk of falls [3]. Adjustment of step width is a primary strategy for maintaining ML balance [4]. Because wider steps improve lateral stability but increase energy expenditure [5], [6], step width should be regulated “as wide as necessary, but no wider”. Thus, the ability to appropriately adjust step width is an important rehabilitation target for independently ambulatory older adults and patients.

Various wearable robots have been developed to facilitate step-width modulation [7], [8]. However, most of these devices employ rigid exoskeletal structures driven by heavy electric motors, which limit backdrivability and hinder the wearer's natural movement. This limitation has motivated the development of soft, lightweight, and flexible wearable robots, namely, exosuits.

Soft exosuits, mainly composed of textiles, aim to reduce mechanical stress on the wearer and have attracted increasing research interest [9]. Studies addressing the ML direction have included assisting hip abduction to reduce knee adduction moments [10] or metabolic cost [11]. However, research on soft exosuits that assist both hip adduction and abduction to actively modulate step width is very limited. This scarcity is partly due to challenges in actuation. The cable-driven systems common in many suits require separate motors for bidirectional movements like abduction and adduction, which complicates the hardware design. On the other hand, soft pneumatic exosuits, which use pneumatic artificial muscles (PAMs), have also been proposed [12]. PAMs offer a high power-to-weight ratio while keeping the hardware simple. However, their strong nonlinearity and hysteresis pose a significant challenge to the accurate modeling required for precise, model-based control, thereby limiting related research [13], [14].

The Human-in-the-Loop (HIL) approach offers a solution to the aforementioned challenge of complex exosuit modeling. This method achieves personalized assistance by estimating unknown control parameters in real-time during gait assistance, based on physiological signals or output errors. One study reduced metabolic cost by 17.4 % by optimizing assistive force using Bayesian optimization (BO) based on respiration-derived metabolic estimates [16]. These studies indicate that the HIL approach is a powerful method for real-time estimation of unknown control parameters and for providing personalized assistance.

B. Purpose of This Paper

This study proposes a control method for a soft exosuit that guides a wearer's step width toward a reference value. We developed a pneumatic soft exosuit that assists hip abduction and adduction using PAMs, and adopted a HIL approach that treats the human–exosuit system as a black box. Specifically, we designed a PI controller that uses step-width error as its input and automatically identifies its gains for each participant via BO [17], [18]. Finally, we validated the effectiveness of the proposed method through experiments with human participants.

Research Questions. This study addresses two key questions:

- **Feasibility of Step-Width Guidance**: Can a soft exosuit guide a wearer's step width toward a reference value?

*This work was supported by the Bridgestone Corporation and JSPS KAKENHI Grant Number 25K14762.

† Equal contribution

[1]J. Kamimura, T. Miyazaki and K. Kawashima are with Department of Information Physics and Computing, Graduate School of Information Science and Technology, The University of Tokyo, Japan. 5158231060kj at g.ecc.u-tokyo.ac.jp

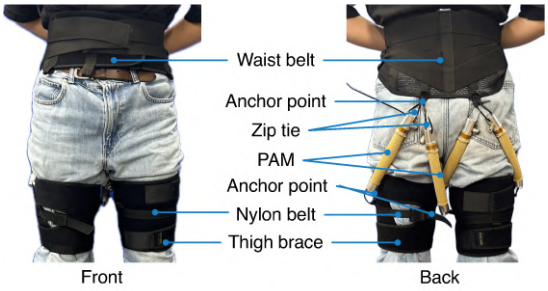

Fig. 1. Developed soft pneumatic exosuit, which assists hip abduction and adduction motion.

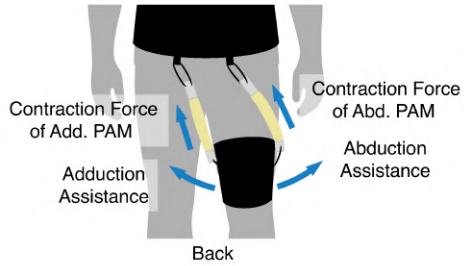

Fig. 2. The soft pneumatic exosuit assists the wearer's hip movements. For clarity, the figure only displays the two PAMs contributing to the right leg's abduction and adduction motions. The assistance is symmetrical for the left leg.

- **PAM Control Strategy**: How should the supply pressure of PAMs be controlled to achieve this guidance?

Contributions. The main contributions of this work are:

- **Bidirectional Soft Exosuit**: Development of a pneumatic soft exosuit capable of assisting hip abduction and adduction, enabling step-width modulation.
- **HIL-Based Gain Tuning**: A control method that uses a Human-in-the-Loop framework with Bayesian optimization to automatically tune PI gains, treating the human–exosuit system as a black box.

II. DEVICE AND METHOD

A. Soft Pneumatic Exosuit

Fig. 1 shows the developed soft pneumatic exosuit driven by PAMs. The four PAMs are attached to the wearer's thighs, and their contraction force assists the wearer's hip abduction and adduction motions, as shown in Fig. 2. This motion assistance guides the wearer's step width toward a reference value. The PAMs were made by the Bridgestone Corporation, and their diameter is 25 mm, their length is 150 mm, and their weight is 123.0 g.

The textile components of the soft exosuit consist of a waist belt (MEDIAID; mass, 269.5 g) and two thigh supporters (EXCITESPORTS; mass, 202.5 g). To transmit the PAM tension to the wearer's body, anchor tags are sewn onto each textile component at positions empirically determined to be effective for providing abduction and adduction assistance during the swing phase. The actuators are secured by connecting these tags to the end-fittings of the PAMs using zip ties.

The total mass of the wearable components is 1.175 kg, which mitigates the physical load on the wearer. A unique feature of this soft exosuit is the absence of electrical sensors on the wearable components. This feature enhances the soft exosuit's usability by eliminating the need for sensor calibration and simplifying the donning process. The control system of the soft exosuit is described in detail in the following section.

B. Step Width Controller

In this study, we designed a PI controller to guide the wearer's step width to a reference value. The controller uses the error between the measured and reference lateral position of each foot as input to determine the supply pressure to the PAMs.

The control variables were measured using an optical motion capture system (Fig. 3). Markers were attached to the navel, hips, knees, ankles, and toes. The controller input, the lateral foot position $y^*(t)$, was defined as the mediolateral coordinate of the toe in a trunk-centered frame whose origin was the navel. The reference lateral position $y^*_{\mathrm{ref}}(t)$ was set symmetrically about the trunk centerline, and the step-width error was defined as:

$$e^*(t) = y^*_{\mathrm{ref}}(t) - y^*(t), \quad \text{where } * \in \{\mathrm{right}, \mathrm{left}\}. \tag{1}$$

Based on this error $e^*(t)$, the reference pressure values, $p^{*,\,\mathrm{abd}}_{\mathrm{ref}}(t)$ and $p^{*,\,\mathrm{add}}_{\mathrm{ref}}(t)$, are calculated for the two types of PAMs that drive hip abduction and adduction.

This control scheme switches the actuated PAM based on the sign of the step-width error $e^*(t)$ and introduces a deadband so that no assistance is provided when the error is sufficiently small. To describe this behavior, we first define the effective error outside the deadband as

$$e^*_{\mathrm{eff}}(t) = \begin{cases} e^*(t) - \mathrm{sgn}\big(e^*(t)\big)\,\delta, & |e^*(t)| > \delta, \\ 0, & |e^*(t)| \le \delta, \end{cases} \tag{2}$$

where $\delta = 0.025$ m is the deadband width. When $e^*_{\mathrm{eff}}(t) > 0$, the controller drives the abduction PAM; when $e^*_{\mathrm{eff}}(t) < 0$, it drives the adduction PAM.

During the swing phase of the k-th step, from $t_{\mathrm{start},k}$ to $t_{\mathrm{end},k}$, the selective activation of each PAM is represented by the gating functions

$$\Gamma^+_k(t) = \begin{cases} 1, & t_{\mathrm{start},k} \le t < t_{\mathrm{end},k} \text{ and } e^*_{\mathrm{eff}}(t) > 0, \\ 0, & \text{otherwise}, \end{cases} \tag{3}$$

$$\Gamma^-_k(t) = \begin{cases} 1, & t_{\mathrm{start},k} \le t < t_{\mathrm{end},k} \text{ and } e^*_{\mathrm{eff}}(t) < 0, \\ 0, & \text{otherwise}, \end{cases} \tag{4}$$

so that at most one PAM is active at any time and both PAMs are inactive during stance.

Using these definitions, the reference pressures for the abduction and adduction PAMs are given by the following PI control law:

$$p^{*,\mathrm{abd}}_{\mathrm{ref}}(t) = \Gamma^+_k(t)\left(K_{\mathrm{P}} e^*_{\mathrm{eff}}(t) + K_{\mathrm{I}} I^+_k(t)\right), \tag{5}$$

$$p^{*,\mathrm{add}}_{\mathrm{ref}}(t) = \Gamma^-_k(t)\left(-K_{\mathrm{P}} e^*_{\mathrm{eff}}(t) + K_{\mathrm{I}} I^-_k(t)\right), \tag{6}$$

where the integral terms accumulate the effective error only while each PAM is active:

$$I^\pm_k(t) = \int_{\tau^\pm_k(t)}^{t} \Gamma^\pm_k(\tau)\left(\pm e^*_{\mathrm{eff}}(\tau)\right) \mathrm{d}\tau, \tag{7}$$

$$\tau^\pm_k(t) = \sup\left\{\tau \le t \,\middle|\, \tau \in [t_{\mathrm{start},k}, t_{\mathrm{end},k}),\ \Gamma^\pm_k(\tau) = 0\right\}, \tag{8}$$

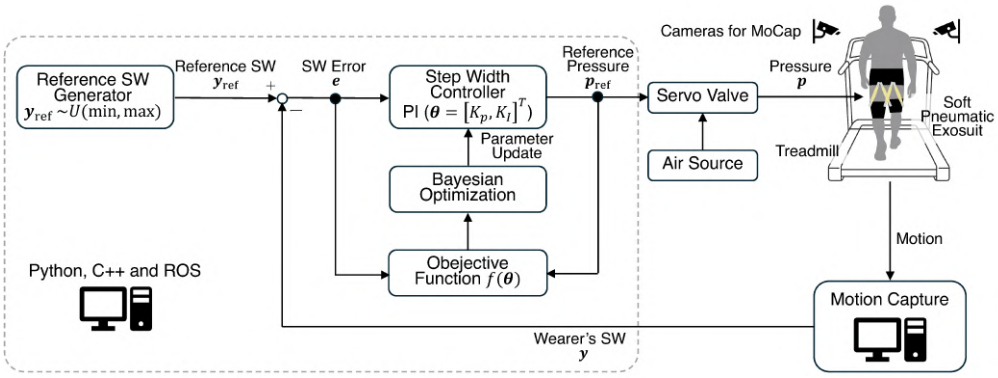

Fig. 3. An overview of the proposed Human-in-the-Loop system. The Reference Step Width (SW) Generator generates a reference step width from a uniform distribution and determines the corresponding reference leg position, $\boldsymbol{y}_{\mathrm{ref}} = [y_{\mathrm{ref}}^{\mathrm{right}},\ y_{\mathrm{ref}}^{\mathrm{left}}]^T$. Based on the error, $\boldsymbol{e} = [e^{\mathrm{right}},\ e^{\mathrm{left}}]^T$, between the leg position of the wearer, $\boldsymbol{y} = [y^{\mathrm{right}},\ y^{\mathrm{left}}]^T$, measured by motion capture, and this reference, the Step Width Controller outputs a reference pressure, $\boldsymbol{p}_{\mathrm{ref}} = [p_{\mathrm{ref}}^{\mathrm{right,\ add}},\ p_{\mathrm{ref}}^{\mathrm{left,\ add}},\ p_{\mathrm{ref}}^{\mathrm{right,\ abd}},\ p_{\mathrm{ref}}^{\mathrm{left,\ abd}}]^T$, to the soft pneumatic exosuit. Bayesian Optimization then optimizes the PI gains, $\boldsymbol{\theta} = [K_{\mathrm{P}},\ K_{\mathrm{I}}]^T$, for each wearer by minimizing the objective function, $f(\boldsymbol{\theta})$.

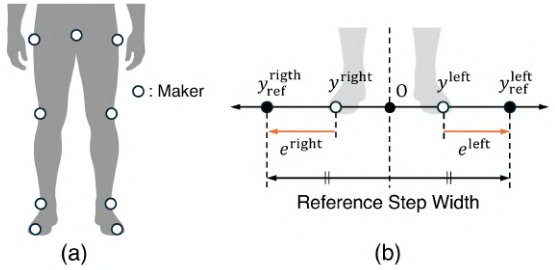

Fig. 4. (a) Motion capture markers used to estimate posture. (b) Definition of the step-width error.

which resets the integral at each activation of the corresponding PAM. During the stance phase, $\Gamma_k^+(t)$ and $\Gamma_k^-(t)$ are zero, and the reference pressures and integral states are set to zero, where K_{P} [kPa/m] and K_{I} [kPa/(m·s)] denote the proportional and integral gains, and $t_{\mathrm{start},k}$ [s] and $t_{\mathrm{end},k}$ [s] are the start and end times of the k-th swing phase.

C. Objective Function for Optimization

In this control system, the magnitude of the haptic feedback that guides the wearer's step width to a reference value is adjusted by the PI gains, $\boldsymbol{\theta} = [K_{\mathrm{P}},\ K_{\mathrm{I}}]^T$. Therefore, a quantitative evaluation metric is required to identify wearer-specific gains $\boldsymbol{\theta}$. In this study, the objective function $f(\boldsymbol{\theta})$ was defined as a quantitative evaluation metric. This function was designed to assess two aspects: (1) the control performance in guiding the wearer's step width toward the reference trajectory, and (2) the ability to prevent excessive increases in the reference pressure. To mitigate the influence of instantaneous fluctuations in the evaluation values, the objective function was computed as the time-averaged value over the entire evaluation period. The function is expressed as follows:

$$f(\boldsymbol{\theta}) = \frac{1}{N}\sum_{i=1}^{N}\left(w_e\|\boldsymbol{e}(t_i)\|_2^2 + w_p\left\|\max\left(\mathbf{0},\ \boldsymbol{p}_{\mathrm{ref}}(t_i;\boldsymbol{\theta}) - p_{\mathrm{lim}}\mathbf{1}\right)\right\|_2^2\right), \tag{9}$$

where N is the number of samples collected during the evaluation period; $\boldsymbol{e} = [e^{\mathrm{right}}, e^{\mathrm{left}}]^T$ is the step-width error vector; and $\boldsymbol{p}_{\mathrm{ref}} = [p_{\mathrm{ref}}^{\mathrm{right,\ add}},\ p_{\mathrm{ref}}^{\mathrm{left,\ add}},\ p_{\mathrm{ref}}^{\mathrm{right,\ abd}},\ p_{\mathrm{ref}}^{\mathrm{left,\ abd}}]^T$ is the reference pressure vector. The weighting coefficients w_e and w_p were determined experimentally to be $w_e = 10^3$ and $w_p = 10^{-5}$. $p_{\mathrm{lim}} = 500$ kPa denotes the upper limit of the reference pressure, and $\mathbf{1}$ is a vector whose elements are all one. A smaller value of $f(\boldsymbol{\theta})$ indicates a better set of parameters.

D. Bayesian Optimization

In this study, we aim to optimize the PI control gains $\boldsymbol{\theta} = [K_{\mathrm{P}}, K_{\mathrm{I}}]^T$ based on the objective function $f(\boldsymbol{\theta})$ defined in Section II-C. To achieve this, we adopted BO, a method well suited for finding the global optimum of expensive-to-evaluate objective functions within a limited number of trials. The parameter search domains were set to $K_{\mathrm{P}} \in [0, 20203]$ and $K_{\mathrm{I}} \in [0, 34358]$. These bounds were determined such that the reference pressure p_{ref} would not exceed the upper limit p_{lim} even when only the proportional or the integral term was active. Specifically, the upper bounds were defined based on the standard deviation of the step width observed at a large step-width condition [19].

In our BO framework, we used a Gaussian process (GP) as a surrogate model for the objective function. We assume that our observation of the objective function, y, is the true function value, $f(\boldsymbol{\theta})$, corrupted by an additive noise term that follows a Gaussian distribution with a mean of zero and a variance of $\sigma_{\mathrm{noise}}^2$. This observation model is expressed as follows:

$$y = f(\boldsymbol{\theta}) + \varepsilon, \quad \text{where } \varepsilon \sim \mathcal{N}(0, \sigma_{\mathrm{noise}}^2). \tag{10}$$

To define the GP prior, we adopted the anisotropic radial basis function kernel, a standard approach [18], to account for the assumed different scales of influence of the gains K_{P} and K_{I} on the objective function. The kernel function is expressed as follows:

$$k(\boldsymbol{\theta}, \boldsymbol{\theta}') = \sigma_{\mathrm{signal}}^2 \exp\left(-\frac{1}{2}(\boldsymbol{\theta} - \boldsymbol{\theta}')^T \boldsymbol{\Lambda}^{-1}(\boldsymbol{\theta} - \boldsymbol{\theta}')\right), \tag{11}$$

where $\sigma_{\mathrm{signal}}^2$ is the signal variance, and $\boldsymbol{\Lambda} = \mathrm{diag}(l_{\mathrm{P}}^2, l_{\mathrm{I}}^2)$ is a diagonal matrix containing the squared length scale, l, for each dimension. The GP hyperparameters,

$[\sigma^2_{\text{signal}},\ l_{\text{P}},\ l_{\text{I}},\ \sigma^2_{\text{noise}}]$, were updated each time a new data point was added by maximizing the log marginal likelihood.

The next gain to be evaluated, $\boldsymbol{\theta}_{n+1}$, was selected as the point that maximizes the acquisition function, which was chosen to be the Expected Improvement (EI) [18]. The EI is given by the following closed-form expression:

$$EI(\boldsymbol{\theta}) = (f_{\min} - \mu_n(\boldsymbol{\theta}))\Phi(Z) + \sigma_n(\boldsymbol{\theta})\phi(Z), \qquad (12)$$

where

$$f_{\min} = \min_{i=1,\ldots,n} f_i,\ Z = \frac{f_{\min} - \mu_n(\boldsymbol{\theta})}{\sigma_n(\boldsymbol{\theta})},$$

and, $\mu_n(\boldsymbol{\theta})$ and $\sigma_n(\boldsymbol{\theta})$ are the posterior mean and standard deviation of the GP at a candidate point $\boldsymbol{\theta}$, respectively; and $\Phi(\cdot)$ and $\phi(\cdot)$ are the cumulative distribution function and probability density function of the standard normal distribution, respectively.

III. EXPERIMENT WITH HUMAN PARTICIPANTS

A. Participants

Two healthy male adults ($n = 2$; age, 23.5 ± 0.7 years; mass, 57.0 ± 1.4 kg; height, 1.71 ± 0.01 m; mean $\pm$ S.D.) participated in this study. The study was approved by the Ethics Committee of the Graduate School of Information Science and Technology, The University of Tokyo (Approval No. UT-IST-RE-250402-2), and all participants provided informed consent prior to the experiment.

B. Experimental Setup

In this study, the device's PAMs were connected to pneumatic servo valves (Festo, MPYE-5-1/4-010-B) via polyurethane tubes with a length of 4.5 m (PISCO, UBT series), which controlled the amount of air supplied to the PAMs. The participant's motion was measured at a sampling frequency of 500 Hz using a six-camera motion capture system (Qualisys, Miqus M3 camera). Participants walked on a fixed-speed treadmill (Circle Fitness) during the measurements. Markers were attached to the participant's body at the same locations as described in Section II-B. The 3D coordinates of the markers were measured in real time by the motion capture system's dedicated software and transmitted to a control PC via a TCP/IP network. Additionally, four pressure sensors (SMC, PSE510) were used to measure the internal pressure of the PAMs. The entire control software was developed on the control PC using Python, C++, and ROS (Robot Operating System). BO was implemented using GPyOpt [20].

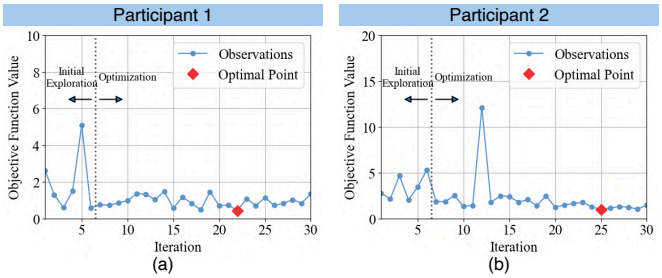

Fig. 5. Progression of the observed objective function values versus the number of iterations. (a) shows the data for participant 1 and (b) for participant 2.

TABLE I

OPTIMIZED GAINS $\boldsymbol{\theta}^*$ AND BEST INITIAL EXPLORATION GAINS $\boldsymbol{\theta}_{\text{init}}$.

Participant	Optimized $\boldsymbol{\theta}^*$		Initial $\boldsymbol{\theta}_{\text{init}}$	
	K_{P} [kPa/m]	K_{I} [kPa/(m·s)]	K_{P} [kPa/m]	K_{I} [kPa/(m·s)]
1	7.68×10^3	1.17×10^4	1.12×10^4	1.30×10^4
2	4.65×10^3	8.76×10^3	1.24×10^4	7.82×10^3

C. Experimental Protocol

The experiment consisted of three sessions conducted on a single day: familiarization, parameter tuning, and validation. All trials were conducted at a constant speed of 1.11 m/s for all participants.

First, in the familiarization session, participants wore the soft exosuit and walked on the treadmill. The soft exosuit was controlled using the PI gains that had been pre-optimized for the author through preliminary experiments with BO. This session continued until each participant verbally reported that they had sufficiently adapted to the device's assistance.

Subsequently, in the parameter tuning session, the PI gains were adjusted via BO. Participants were instructed beforehand to adjust their step width while walking, following the guidance from the external forces applied by the soft exosuit. During this period, the reference step width changed uniformly at random every ten seconds within a range of $[0.15, 0.35]$ m. A five-minute rest followed, during which participants remained in the soft exosuit.

Finally, the validation session compared three conditions to assess the controller's effectiveness: "Optimized Assistance", "Initial Assistance", and "No Assistance". In the first two conditions, the exosuit provided haptic guidance using either the optimized gains $\boldsymbol{\theta}^*$ or the best gains from the initial exploration, $\boldsymbol{\theta}_{\text{init}}$. In the No Assistance condition, participants manually adjusted their step width to match a verbally presented reference without assistance. Before the No Assistance condition, participants visually confirmed the reference step-width range, $[0.15, 0.35]$ m, using a ruler placed at their feet. Each condition included three 3.5-min trials, and the order of conditions was counterbalanced to minimize order effects.

The evaluation method was to calculate the root mean square error (RMSE) between the measured step width and the presented reference value for each condition. In addition, to examine whether the soft exosuit influenced other gait parameters beyond step width, step length was also evaluated. In each condition, participants performed 3.5-min trials, and the central 3.0 min of each trial was used as the analysis interval.

IV. RESULTS AND DISCUSSION

A. Optimization of PI Gains

Fig. 5 shows the progression of the observed values of the objective function versus the number of iterations for participants 1 and 2 during the parameter tuning session. After the six initial exploration iterations, the optimization

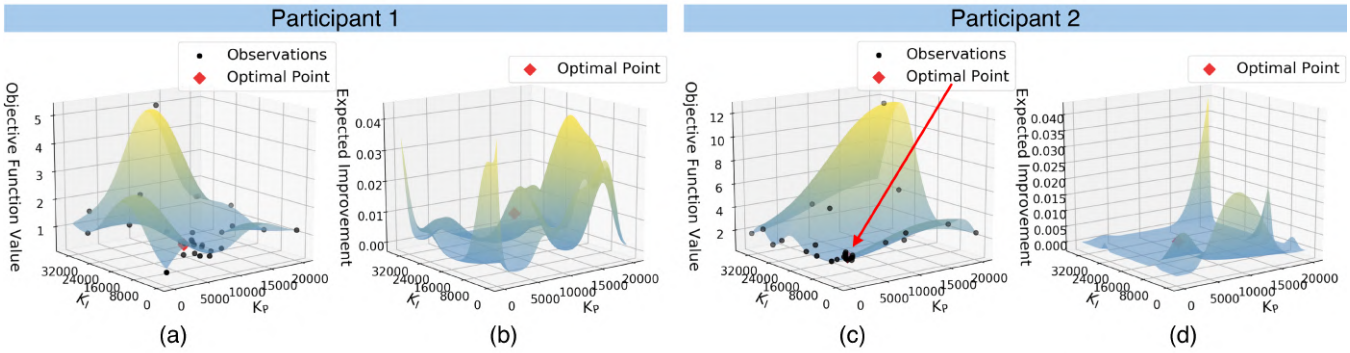

Fig. 6. Predicted response surface and Expected Improvement (EI) of the objective function $f(\boldsymbol{\theta})$ for participants 1 and 2 at the final iteration. (a) and (c) show the observed values and the predicted response surface of the objective function $f(\boldsymbol{\theta})$ while (b) and (d) show the corresponding EI.

TABLE II

RMSE OF STEP WIDTH UNDER EACH CONDITION.

Participant		Step-Width RMSE [m] (↓)		
		Optimized $\boldsymbol{\theta}^*$	Initial $\boldsymbol{\theta}_{\text{init}}$	No Assistance
1	Mean	**0.0588**	0.0611	0.1039
	S.D.	0.0039	0.0013	0.0039
2	Mean	**0.0555**	0.0561	0.0758
	S.D.	0.0016	0.0027	0.0044

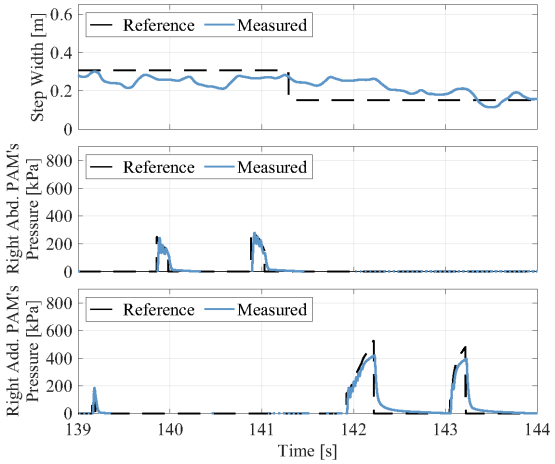

Fig. 7. Time-series data of the step-width error and the supply pressure to the right-leg PAMs of the device.

was performed, and the minimum value of the function was progressively updated. However, the fact that the observed values do not decrease monotonically suggests that the acquisition function, EI, functioned as intended by balancing the trade-off between exploration and exploitation.

The final predicted response surface of the objective function $f(\boldsymbol{\theta})$ is shown in Fig. 6. The surface confirms that the optimal gain $\boldsymbol{\theta}^*$ differed between participants. In regions where K_{p} and K_{I} are large, the objective function increases, indicating that parameter combinations causing the reference pressure to exceed its upper limit were effectively penalized. Furthermore, the concentration of sampled points around the optimal point in the parameter space demonstrates that BO efficiently explored its vicinity.

B. Validation of Controller

Table II summarizes the step-width RMSE during the validation session. For both participants, the assisted conditions—Optimized Assistance and Initial Assistance —substantially reduced RMSE compared with the No Assistance

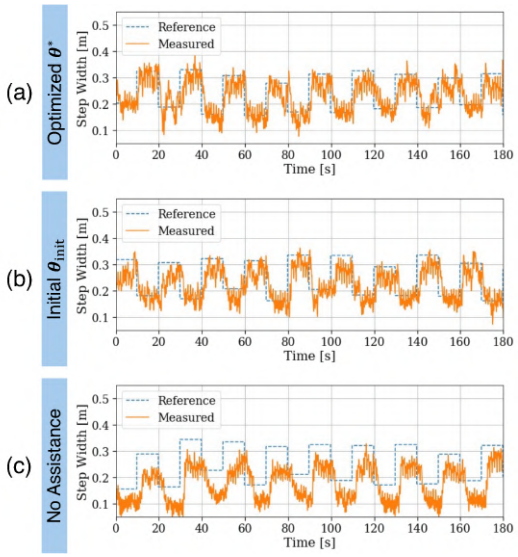

Fig. 8. Time-series data of the reference and measured step width for Participant 1 during the validation session. Subplots (a), (b), and (c) show the Optimized Assistance, Initial Assistance, and No Assistance conditions, respectively.

condition. Specifically, Optimized Assistance decreased the mean RMSE relative to No Assistance by 43.4 % for Participant 1 and 26.8 % for Participant 2, and Initial Assistance achieved comparable reductions. These improvements are large compared with the trial-to-trial standard deviations, indicating a robust effect of the exosuit assistance on step-width tracking accuracy. In contrast, the comparison between Optimized Assistance and Initial Assistance shows a consistent but more modest advantage of Optimized Assistance: the mean RMSE was reduced by 3.76 % for Participant 1 and 1.07 % for Participant 2, which is comparable to the within-condition variability. Nevertheless, the consistent trend across both participants suggests that Bayesian optimization can refine the promising gains obtained from the initial exploration and further improve tracking performance, a possibility that will be examined more rigorously in future experiments with a larger sample size.

Furthermore, Fig. 7 verifies that the PI controller functioned as intended. The appropriate switching and shape of the pressure waveforms, along with adherence to the 500 kPa pressure limit, confirm that both the control logic and the objective function's penalty term were effective.

Fig. 8 presents representative time-series data of the ref-

erence and measured step widths for Participant 1 under the three conditions. In both Optimized Assistance and Initial Assistance, the measured step width closely follows the reference with only a small steady-state error, whereas in the No Assistance condition a noticeable residual error remains, particularly for larger reference step widths. The waveforms of Optimized Assistance and Initial Assistance are qualitatively similar, indicating that both gain settings enable accurate tracking for this participant, with only minor differences consistent with the RMSE results.

Stride-length analysis confirmed that the exosuit did not affect AP-direction gait parameters. Participant 1 showed nearly identical mean stride lengths across all conditions (Opt: 0.6207 m, Init: 0.6213 m, No: 0.6157 m). Participant 2 exhibited similarly consistent means with no notable differences between assistance conditions.

Correlation analysis indicated that stride length and step width were largely independent. Participant 1 showed weak correlations across all conditions (Opt: $r = 0.0280$, Init: $r = 0.0978$, No: $r = 0.0525$). Participant 2 similarly exhibited nearly no correlation in all conditions (Opt: $r = 0.0313$, Init: $r = -0.0117$, No: $r = -0.2014$). Taken together, these results demonstrate that stride length and step width were independent for both participants, with no correlations strong enough to influence overall gait behavior.

V. CONCLUSION

In this study, we developed a soft pneumatic exosuit specialized for hip abduction and adduction assistance, with the objective of guiding a wearer's step width to a reference value during walking. We proposed a HIL approach that optimizes the PI controller gains for each wearer using Bayesian optimization and experimentally validated its effectiveness.

The experimental results from the parameter tuning session demonstrated that the proposed method can automatically identify participant-specific optimal gains, which varied significantly between individuals. In the validation session, Optimized Assistance and Initial Assistance both improved step-width tracking accuracy compared with No Assistance, and Optimized Assistance showed a consistent, though modest, additional reduction in RMSE. These findings demonstrate that the proposed soft pneumatic exosuit combined with the HIL-based gain optimization provides an effective and practical framework for personalized step-width guidance. Looking ahead, this framework could be applied in rehabilitation to train and enhance a wearer ' s step-width adjustment ability, contributing to safer and more stable walking.

VI. ACKNOWLEDGEMENT

We are grateful for Shingo Oono's technical assistance with the Bridgestone Corporation.

REFERENCES

[1] G. S. Sawicki, O. N. Beck, I. Kang, R. P. D'Andrea, and S. H. Collins, "The exoskeleton expansion: improving walking and running economy," J NeuroEngineering Rehabil, vol. 17, no. 25, 2020, doi: 10.1186/s12984-020-00663-9.

[2] M. H. Woollacott and P. F. Tang, "Balance Control During Walking in the Older Adult: Research and Its Implications," Physical Therapy, vol. 77, no. 6, pp. 646–660, Jun. 1997, doi: 10.1093/ptj/77.6.646.

[3] L. Sturnieks, R. St George, and S. R. Lord, "Balance disorders in the elderly," Neurophysiologie Clinique/Clinical Neurophysiology, vol. 38, no. 6, pp. 467–478, 2008, doi: https://api.semanticscholar.org/CorpusID:10370640.

[4] A. D. Kuo, "Stabilization of Lateral Motion in Passive Dynamic Walking," The International Journal of Robotics Research, vol. 18, no. 9, pp. 917–930, 1999, doi: 10.1177/02783649922066655.

[5] M. Bruijn and J. H. van Dieën, "Control of human gait stability through foot placement," Journal of the Royal Society Interface, vol. 15, no. 20170816, 2018, doi: 10.1098/rsif.2017.0816.

[6] A. Winter, "Human balance and posture control during standing and walking," Gait & Posture, vol. 3, no. 4, pp. 193–214, 1995, doi: 10.1016/0966-6362(96)82849-9.

[7] A. Alili, A. Fleming, V. Nalam, M. Liu, J. Dean, and H. Huang, "Abduction/Adduction Assistance From Powered Hip Exoskeleton Enables Modulation of User Step Width During Walking," IEEE Transactions on Biomedical Engineering, vol. 71, no. 1, pp. 334–342, Jan. 2024, doi: 10.1109/TBME.2023.3301444.

[8] T. Zhang, M. Tran, and H. Huang, "Design and Experimental Verification of Hip Exoskeleton With Balance Capacities for Walking Assistance," IEEE/ASME Transactions on Mechatronics, vol. 23, no. 1, pp. 274-285, 2018. doi:10.1109/TMECH.2018.2790358.

[9] A. Rodríguez-Fernández, J. Lobo-Prat, and J. M. Font-Llagunes, "Systematic review on wearable lower-limb exoskeletons for gait training in neuromuscular impairments," J NeuroEngineering Rehabil, vol. 18, no. 22, 2021, doi: 10.1186/s12984-021-00815-5.

[10] J. Park, K. Nam, J. Yun, J. Moon, J. Ryu, S. Park, S. Yang, A. Nasirzadeh, W. Nam, S. Ramadurai, M. Kim, and G. Lee, "Effect of hip abduction assistance on metabolic cost and balance during human walking," Science Robotics, vol. 8, no. 83, p. eade0876, 2023, doi: 10.1126/scirobotics.ade0876.

[11] H. D. Yang, M. Cooper, A. Eckert-Erdheim, D. Orzel, and C. J. Walsh, "A Soft Exosuit Assisting Hip Abduction for Knee Adduction Moment Reduction During Walking," IEEE Robotics and Automation Letters, vol. 7, no. 3, pp. 7439–7446, Jul. 2022, doi: 10.1109/LRA.2022.3182106.

[12] T. Miyazaki, T. Kawase, T. Kanno, M. Sogabe, Y. Nakajima, and K. Kawashima, "Running Motion Assistance Using a Soft Gait-Assistive Suit and Its Experimental Validation," IEEE Access, vol. 9, pp. 94700–94713, 2021, doi: 10.1109/ACCESS.2021.3093209.

[13] B. Kalita, A. Leonessa, and S. K. Dwivedy, "A Review on the Development of Pneumatic Artificial Muscle Actuators: Force Model and Application," Actuators, vol. 11, no. 10, p. 288, 2022, doi: 10.3390/act11100288.

[14] M. Van Damme, D. Lefeber, J. De Schutter, and H. Van Brussel, "Modeling Hysteresis in Pleated Pneumatic Artificial Muscles," in 2008 IEEE Conference on Robotics, Automation and Mechatronics, 2008, pp. 471–476, doi: 10.1109/RAMECH.2008.4681431.

[15] Z. Li, Q. Li, P. Huang, H. Xia, and G. Li, "Human-in-the-Loop Adaptive Control of a Soft Exo-Suit With Actuator Dynamics and Ankle Impedance Adaptation," IEEE Transactions on Cybernetics, vol. 53, no. 12, pp. 7920-7932, 2023. doi:10.1109/TCYB.2023.3240231.

[16] Y. Ding, G. B. G. Panizzolo, J. P. E. G. van den Bogert, A. D. Kuo, and C. J. Walsh, "Human-in-the-loop optimization of hip assistance with a soft exosuit during walking," Science Robotics, vol. 3, no. 23, p. eaar5438, 2018, doi: 10.1126/scirobotics.aar5438.

[17] D. R. Jones, M. Schonlau, and W. J. Welch, "Efficient Global Optimization of Expensive Black-Box Functions," Journal of Global Optimization, vol. 13, pp. 455–492, 1998, doi: 10.1023/A:1008306431147.

[18] E. Brochu, V. M. Cora, and N. de Freitas, "A Tutorial on Bayesian Optimization of Expensive Cost Functions, with Application to Active User Modeling and Hierarchical Reinforcement Learning," CoRR, vol. abs/1012.2599, 2010.

[19] J. A. Perry and M. Srinivasan, "Walking with wider steps changes foot placement control, increases kinematic variability and does not improve linear stability," Royal Society Open Science, vol. 4, no. 6, p. 160627, 2017. doi: 10.1098/rsos.160627.

[20] The GPyOpt authors, "GPyOpt: A Bayesian Optimization framework in python," 2016. [Online]. Available: http://github.com/SheffieldML/GPyOpt.